GaInNAs(Sb) long wavelength communications lasers

J.S. Harris, Jr., S.R. Bank, M.A. Wistey and H.B. Yuen

Abstract: Dilute nitride GaInNAs and GaInNAsSb alloys grown on GaAs have quickly become excellent candidates for a variety of lower cost 1.2–1.6 μm lasers, optical amplifiers and high-power Raman pump lasers that will be required to power the Internet and advanced communications systems capable of delivering multi-Gbit/s data rates to the desktop. Two particularly critical devices are vertical-cavity surface-emitting lasers (VCSELs) which must operate at high data rates (≥ 10 Gbit/s), uncooled over a broad thermal operating range and high power (≥ 500 mW) edge-emitting lasers for Raman amplifier pumps. Despite the fact that these materials are grown in a metastable regime, and there are still many remaining challenges, progress has been both rapid and very promising. Some of the material challenges include the limited solubility of N in GaAs, nonradiative defects that are caused by either or a combination of N incorporation, low growth temperature, and ion damage from the N plasma source. N and Sb add a unique set of properties to this metastable alloy; however, this significantly increases the complexity of its characterisation. The addition of Sb significantly improves the epitaxial growth and optical properties of the material at wavelengths longer than 1.3 μm and broadens the range of In and N composition alloys that can be grown. By adding Sb to the alloy, luminescence has been greatly enhanced between 1.3 and 1.6 μm where normally poor quality material results. Progress in overcoming some of the material challenges is described, particularly GaAsNSb against GaNAs QW barriers, plasma-source ion damage and progress in realising record-setting edge-emitting lasers and the first VCSELs operating at 1.5 μm based on GaInNAsSb QWs grown by solid-source MBE on GaAs.

1 Introduction

In spite of the incredibly rapid growth and capacity of current optical communications networks and the Internet, it should come as little surprise that they are now limited by the same problems of all mature, high-speed transportation systems, such as airlines, trains and automobiles: all are limited by the switching hub from the main high speed/capacity backbone through the traffic jams in the on/off ramps and slow feeder lines to the final destination illustrated in Fig. 1. This bottleneck on the information highway is often referred to as the 'last mile' problem and is now the focus of considerable effort to create truly high-speed metro (MAN) and local (LAN) area networks [1, 2]. This is the driving force behind the development of low-cost, 1.3–1.6 μm, directly modulated, uncooled vertical-cavity surface-emitting lasers (VCSELs) because in contrast to the backbone, where there are tens of thousands of lasers and performance rather than cost is the critical issue, high-speed direct access will require tens to hundreds of million lasers. For the high-speed LANs and MANs required to deliver 'fibre to the desktop', total system cost becomes dominated by the end terminal cost and today that is driven by the lasers. Thus, laser cost is the major issue before widespread adoption is embraced. Compared to current generation lasers, the cost will have to be reduced by at least 100 times. While this might seem a very daunting challenge, first-generation LANs based on low cost 850 nm GaAs VCSELs have demonstrated that they can meet the cost, reliability, speed and thermal requirements for such lasers, the only problem being that they operate at the wrong wavelength and 10 Gbit/s transmission is only possible over about 50 m (not km!) [1–3]. Thus, longer wavelength lasers are absolutely essential to achieve useful transmission distances at this data rate. For long-haul applications, 1.55 μm InGaAsP/InP-based Bragg grating and distributed feedback (DFB) lasers are commonly used, but they are prohibitively expensive for high-volume MAN and LAN systems. Despite sizeable efforts to realise low-cost, long wavelength VCSELs, limitations in the current alloy systems have made this an extremely difficult challenge.

In the past few years, a new material system has been investigated which has the potential to make long-wavelength low-cost VCSELs a reality. GaInNAs, which can be grown nearly lattice-matched to GaAs, was found to have a bandgap in the telecommunication wavelength range [1–4] and recently commercial 1.28 μm VCSELs have been described [5]. Being grown on GaAs gives this system the distinct advantage of being compatible with monolithic growth of GaAs/AlAs distributed Bragg reflecting (DBR) mirrors and a significantly better developed fabrication technology owing to the unique property of AlAs oxidation. Other advantages compared to InP-based solutions include better thermal stability, owing to larger conduction band offsets between barrier and quantum well (QW), and simplified compositional control over As/P mixed group-V solutions. While growth of GaInNAs QWs allows fabrication of near 1.3 μm VCSELs, manufacturers are

IEE Proceedings online no. 20040937

doi: 10.1049/ip-opt:20040937

Paper first received 7th June and in revised form 16th June 2004

The authors are with the Solid State and Photonics Lab, Stanford University, CIS-X 328, Via Ortega, Stanford, CA 94305-4075, USA

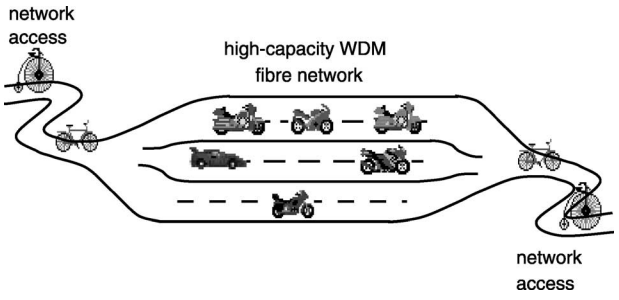

Fig. 1 *Cartoon illustrating the on/off ramp bottlenecks for both highway and 'information highway' transportation systems*

hedging on going clear out to 1.3 μm; for good reason, as they have had yield problems similar to our observed growth sensitivity for these QW alloys and their reproducibility, which is certainly somewhat problematical. We have found that by incorporating Sb to form a quinary alloy GaInNAsSb, the growth window for good 2-D epitaxy is not only expanded, but has enabled the realisation of 1.5 μm low-threshold current, high-power edge-emitting lasers [6, 7] and the first monolithic 1.5 μm VCSELs on GaAs [8]. The major appeal of this quinary alloy is thus a *single* materials system for growth and processing which can produce not only the entire range of devices but enables significant integration of devices with photonic crystal waveguides and resonators, which will be the foundation technology for truly low-cost, high-speed photonic integrated circuits that can provide high bandwidth networks to the desktop [1, 2].

2 Molecular beam epitaxial growth

Owing to the difficulties of incorporating sufficient N in solid solution, growth of GaInNAs and GaInNAsSb are substantially different from all earlier III–V systems [1, 2]. Differences in crystal structure between GaInN and GaInAs, the small size of N compared with As and the high electronegativity of N cause a large miscibility gap between GaInAs and GaInN. In order to grow a homogeneous alloy of GaInNAs or GaInNAsSb, growth must take place under metastable conditions. GaInNAs and GaInNAsSb have been grown by solid-source molecular beam epitaxy (MBE) with a reactive N RF plasma. A plasma source puts out a variety of species (N_2^+, N^+, N as well as electrons and each of the molecular species in excited states), and exactly which species are incorporated and the potential for ion and/or electron damage are still poorly understood [9, 10]. We have now examined a number of these issues and find that the source operation condition and substrate temperature are the most critical parameters for metastable growth of high-quality materials. We use low temperatures, around 425 °C, in order to inhibit phase segregation and improve surface morphology, and a bias voltage applied to the deflection plates of our plasma source to minimise ion damage. Dimeric As and monomeric Sb are supplied using thermal cracking cells. Arsenic overpressure was generally fixed at 15–20 times the group-III flux during growth, unless otherwise noted. A very important property of nitride growth by MBE is the fact that N incorporates with nearly unity sticking conditions, i.e. the group-III growth rate and not the V–V ratio control the N incorporation [11].

One of the major challenges for growth of GaInNAs is avoiding phase segregation and maintaining good 2-D epitaxial growth for materials operating approaching or beyond 1.3 μm as illustrated in Fig. 2. This illustrates a

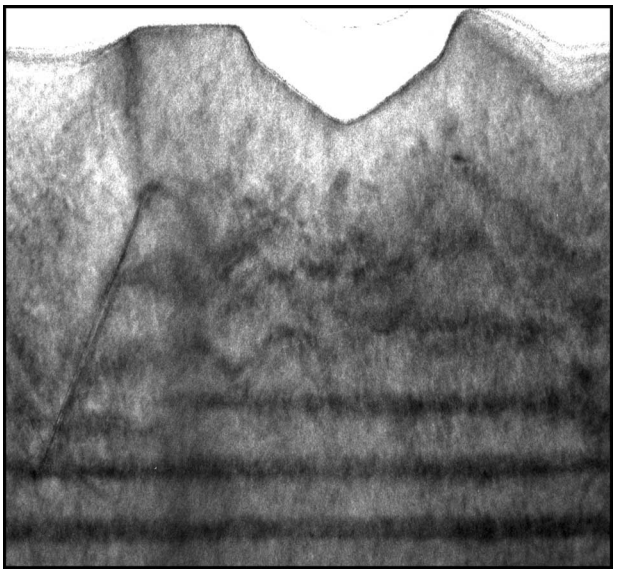

Fig. 2 *TEM cross-section image of 3-QW 35% In GaInNAs–GaAs barrier sample where 3-D growth and phase segregation have occurred in the 3rd QW*

common observation that the first or second QWs grow without phase segregation, but by the third QW, the top interface clearly has regions such as quantum dots and phase segregation. This is also immediately visible with RHEED during growth. TEM characterisation of these regions indicates that they are the result of In migration and local increase in In composition [12].

Growth of GaNAs and GaInNAs both suffer to some degree with the problem illustrated in Fig. 2. Even though GaNAs clearly has no In, N segregation or strain-induced 3-D islanding must be occurring. In an effort to improve material quality, Shimizu *et al.* [13] and Yang *et al.* [14] discovered that Sb could be used as a surfactant in InGaAs and GaInNAs growth, respectively. When we introduced Sb into the growth of GaInNAs, we observed a significant enhancement of PL, particularly at wavelengths greater than 1.3 μm as illustrated in Fig. 3 [1, 2, 6]. However, we quickly discovered that Sb acts as both a surfactant and constituent when used in GaInNAs, forming GaInNAsSb [6, 15]. Until

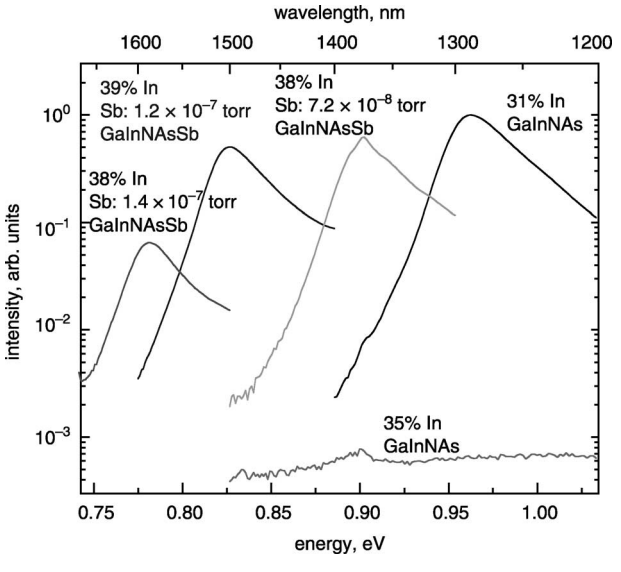

Fig. 3 *Photoluminescence of GaInNAs(Sb) comparing the best 1.3 μm material grown without Sb and the dramatic improvement in PL at even longer wavelengths by adding Sb*

recently, our devices utilising GaInNAsSb as the quantum well (QW) material used GaNAsSb as the barrier material [6, 16, 17]. Sb was incorporated into the barriers because it was thought to be a surface surfactant that would remain on the surface during QW and barrier growth, even if the Sb shutter was closed. It also seemed that it might improve the quality of GaNAs and the interfaces between the QWs and barriers. Although GaInNAsSb has been extensively studied as a quantum well material, there has been very little work reported on GaNAsSb [18, 19].

Because of the rather extensive recent reviews of GaInNAs growth and lasers, we concentrate on recent studies on the effect of growth conditions, including the N RF plasma source, on the materials properties of GaNAsSb and GaInNAsSb, which have been key to producing lasers operating at record long wavelength. The improvements in materials growth have focused on (i) growth temperature and the properties of GaNAs against GaNAsSb as barriers for GaInNAsSb QWs for lasers operating in the 1.3–1.55 μm range; and (ii) the N RF plasma source, species it produces and possible ion damage created during growth of the epitaxial layers. Reflection high-energy electron diffraction (RHEED), high-resolution X-ray diffraction (HRXRD), photoluminescence (PL) and secondary ion mass spectrometry (SIMS) measurements were obtained to analyse the characteristics of the material.

3 GaNAs against GaNAsSb barriers

GaNAsSb/GaAs QW samples were prepared to study the properties of the GaNAsSb material used in barriers of our previous 1.3 and 1.5 μm laser devices [6, 16, 20]. The barriers themselves were 'converted' into single QW (SQW) samples. A series of samples of 20-nm GaNAs(Sb) QWs with GaAs barriers were grown to examine different growth conditions, such as substrate temperature and As overpressure. The compositions of GaNAs(Sb) were chosen to be similar to those used in our 1.3 and 1.55 μm GaInNAsSb lasers [6, 11, 16]. The N content is predetermined, due to its inverse proportional relationship with the group-III flux, and the Sb flux is unchangeable during growth because it is supplied by an unvalved cracker [5, 19]. These combined conditions do not allow the barrier compositions to be arbitrarily changed.

The GaNAs(Sb) SQWs were all grown at 425 °C (except for the substrate temperature study) and the growth rate was either 0.45 μm/h (to duplicate 1.3-μm QW barriers) or 0.30 μm/h (to duplicate 1.5-μm QW barriers). The composition of N in GaNAs was determined by HRXRD and the compositions of N and Sb in GaNAsSb were determined by SIMS and HRXRD. As mentioned earlier, the QW thicknesses were all 20 nm with 50-nm GaAs capping layers. An As-to-Ga overpressure of 20 times (except during the As overpressure study) and an Sb flux of $0.8–1.0 \times 10^{-7}$ torr beam equivalent pressure (BEP) were supplied during the QW growth.

RHEED patterns were monitored during growth. GaNAs produces a streaky 2×4 surface reconstruction which became spotty almost instantly when the Sb shutter was opened, suggesting the surface quality was not as good as GaNAs. This result was somewhat surprising since previous studies have shown that Sb had the opposite effect with InGaAs and GaInNAs [15, 19]. From RHEED, it appears that the growth surface of GaNAs is smoother than that of GaNAsSb.

For a fixed N flux, varying the growth rate alters the amount of N incorporated [11]. However, for a fixed Sb-to-As flux ratio, variations in the growth rate did not change the Sb composition. Sb incorporation appeared to be independent of altered growth conditions, such as the group-III growth rate and N incorporation, suggesting that the flux ratio of Sb-to-As is the deciding factor in determining the composition. This is different from what is observed for GaAsSb growth where, for fixed Sb-to-As flux ratios, different growth rates lead to different incorporation rates [18, 19]. The increase in N composition in GaNAsSb compared to GaNAs in both conditions was expected and not surprising since this has been reported previously [18, 19]. The mechanism for the increased sticking of N in the material is not known. However, it is thought that the properties of Sb as a 'reactive surfactant' help promote the incorporation of N into GaAs [21, 22]. HRXRD scans showed the GaNAsSb was either lattice-matched to GaAs or was very slightly compressively strained for both compositions. This property is not advantageous when used with highly compressively strained GaInNAsSb QW materials since the barriers do not provide any strain compensation to the active regions. Both compositions of GaNAs showed an appreciable amount of tensile strain. From HRXRD, there does not appear to be any improvement of material quality upon addition of Sb to GaNAs for either set of growth conditions. From the Pendellosung fringes, the interfaces for all materials are of good quality. This could suggest that the GaNAs grown was already of excellent quality, or there simply was no effect upon addition of Sb.

SIMS was performed on the GaNAsSb samples mentioned above. Figure 4 shows the SIMS depth profile for the $GaN_{0.029}As_{0.873}Sb_{0.098}$ sample. Although it is relatively straightforward to obtain depth profiles, attaining exact compositional values requires previous calibration due to artefacts, including matrix effects. The SIMS analysis was calibrated using parameters obtained from previous growth analysed with nuclear reaction analysis Rutherford backscattering (NRA–RBS) for N and particle-induced X-ray emission RBS (PIXE–RBS) for Sb. An interesting feature to note in the SIMS depth profile is the top interface of the GaNAsSb layer. The N and Sb profiles do not end at the same location within the sample. This was determined to be real and not a measurement or sputtering artefact, as it was repeatable within the same sample and observed on all other samples measured with SIMS. Upon examination of the SIMS depth profile, it appears Sb continues to incorporate ~5–7 nm beyond the end of N incorporation. Surfactants tend to float on the growth front and do not

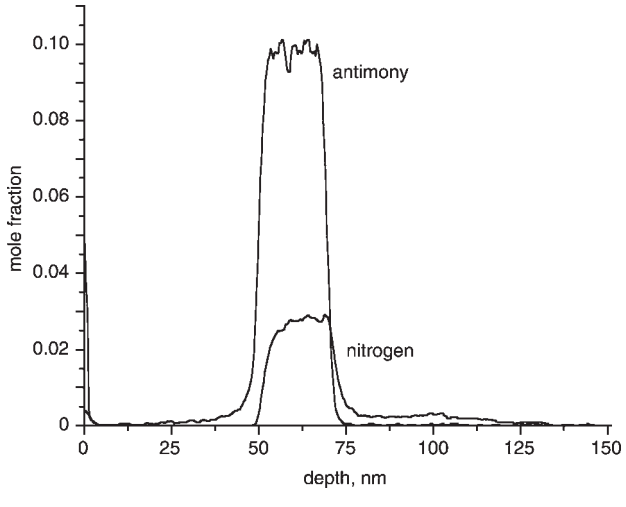

Fig. 4 *Nitrogen and antimony SIMS profiles of $GaN_{0.029}As_{0.873}Sb_{0.098}$ sample illustrating both the incorporation and surface accumulation nature of Sb*

incorporate into the material. As mentioned in earlier papers relating to GaInNAs(Sb), Sb appears to act as a surfactant as well as a group-V component [5, 19]. It is very probable that Sb both incorporates and floats on the growth front of GaNAsSb as well. If this is the case, there will be Sb remaining on the growth front after the shutter is closed to the cell and the residual Sb continues to incorporate or desorb until the supply is exhausted. This growth complication could be quite detrimental to devices, since there is then a thin layer of GaAsSb on top of the QW which could significantly change the originally intended band structure properties due to changes of both composition and strain.

PL measurements were obtained from the $GaN_{0.029}As_{0.873}Sb_{0.098}$ sample. No signal was observed for the $GaN_{0.034}As_{0.867}Sb_{0.099}$ sample, either as-grown or annealed. This suggests the material was of very poor quality and it was not studied further. The PL obtained from the as-grown $GaN_{0.029}As_{0.873}Sb_{0.098}$ sample peaked at 1.316 μm, but was very weak in intensity. This was not surprising since most groups report poor PL intensity for GaInNAs(Sb) samples which have not been annealed [6, 11, 15]. The sample was then annealed at a series of temperatures between 720 °C and 820 °C to study the effect upon the optical quality of the material. Similar to GaInNAs(Sb), annealing the PL samples led to a dramatic increase in PL intensity. The PL intensity increased with increasing annealing temperatures until it peaked at 760 °C and decreased beyond this point. The PL peak wavelength also blue-shifted with increasing anneal temperatures. Compared to the as-grown PL spectrum, the optimal anneal PL signal was 25 times higher in intensity and was blue-shifted 70 nm, which is slightly more than the blue-shift found in GaInNAs(Sb). Unlike GaInNAs(Sb) samples, there is no In in the samples and thus the blue-shifting of the PL wavelength upon annealing cannot be explained by In/Ga/N rearrangement [22–24]. Sources of blue-shifting probably include N outdiffusion, N/As/Sb rearrangement and N declustering. When compared to typical GaInNAs(Sb) PL intensities, the GaNAsSb intensities are at least 25 times lower. The low intensity in comparison to other nitride–arsenides could be due to poor optical quality material or poor band alignment in the active region design. One final point to note is the actual transition energy of the $GaN_{0.034}As_{0.867}Sb_{0.099}$ sample in comparison with the QW material it surrounds in devices. If it is assumed that the PL peak wavelength gives a rough estimate of the bandgap of the material, then it is seen that the bandgap of the $GaN_{0.034}As_{0.867}Sb_{0.099}$ is roughly 0.99 eV while the QW at 1.3 μm is 0.95 eV. With only 40 meV difference in bandgap, there is very poor confinement of electrons and holes within the QW and it is possible that the alignment between the GaNAsSb and GaInNAsSb at 1.3 μm is not the desired type-I alignment.

One of the major questions for quaternary and quinary alloys with three different column-V constituents is their sensitivity to temperature and flux, as this could make compositional control very challenging. In an attempt to study general growth properties of GaNAsSb and potentially improve PL intensity and material quality, a series of samples with varying As-to-Ga overpressures was grown with the same structure as the previous samples. It is known that in mixed group-V materials (AsP or AsSb), the relative fluxes of each group-V element play a large role in composition and growth kinetics. In GaInNAs, there was no significant effect on N incorporation by different As fluxes due to the 'unity' sticking properties of N [11]. However, in GaNAsSb it is suspected that the As and Sb fluxes do indeed affect each other since they do not have the same sticking properties as N. It is also possible that a variation in Sb incorporation could affect the N composition. To test the effects of As overpressure on GaNAsSb, the original 20 times As-to-Ga flux overpressure was varied between 15, 25 and 30 times when growing $GaN_{0.034}As_{0.867}Sb_{0.099}$, the material used as barriers for 1.3 μm QWs. All other growth conditions were held constant. In HRXRD measurements, it was seen that as the As overpressure increased from 15 to 30 times, the strain in the GaNAsSb layer became less compressive. Since this is a quaternary system, it cannot be determined whether the decrease in compressive strain is due to a reduction in Sb concentration, an increase in N concentration, or a combination of both. In all cases, the HRXRD scans did not show any degradation of material compared to the original 20 times sample. To determine the origin of the strain reduction, SIMS was performed to measure the composition. As the As overpressure increased from 15 to 30 times, the Sb concentration drops from 12% to 9%, while the N concentration remains virtually unchanged. This would explain the decrease in compressive strain with increasing As flux, since a reduction in Sb would decrease the lattice constant of GaNAsSb. The increase in As flux thus has a direct effect on the Sb incorporation rate but no discernable effect on N incorporation (as seen in GaNAs) [11]. This decrease in Sb incorporation with increasing As flux is seen commonly in GaAsSb growth [19]. In addition, the change in Sb concentration had no effect on the N incorporation in agreement with previously obtained results [18, 21]. The measurements also show enhanced N incorporation in the GaNAsSb. GaNAs grown under the same growth conditions yields 1.8% N, much lower than the observed 2.4–2.9% in GaNAsSb. The PL intensities are within measurement error and sample repeatability, thus revealing no significant change in optical material quality between the different samples. Going from 15 to 30 times As overpressure, we have only a 3% Sb decrease, thus changing the As overpressure does not have any major effect on GaNAsSb except for the small change in Sb incorporation. The material quality remains the same structurally and optically. For GaInNAs(Sb) QWs with GaNAsSb barriers, it would be beneficial to increase the As overpressure so that the GaNAsSb would have less compressive strain and a larger bandgap for increased confinement in the wells.

The second major growth variable is substrate temperature. The substrate temperature during GaNAsSb growth was also varied to examine the effects on crystal quality and composition. GaInNAs(Sb) was grown at 425 °C to prevent phase segregation and relaxation. One of the driving factors in segregation in GaInNAs(Sb) is the clustering of In-rich areas. The GaNAsSb barriers were also grown at the same temperature, since it was also thought the material would segregate. However, In is not present in this material and this raised the possibility that the material could be grown at a higher temperature. One problem with nitride–arsenide growth is the low substrate temperature. Such low temperatures introduce defects in GaAs, such as As antisites and Ga vacancies, hence it is desirable to grow the material as close to 580 °C as possible to minimise these defects, which may cause nonradiative recombination and reduce luminescence. A series of samples with structures and growth conditions identical to those in the initial study were grown with varying substrate temperatures: +50 °C (475 °C), +100 °C (525 °C) and +150 °C (575 °C). Another set of samples with no Sb (GaNAs) was also grown for comparison. HRXRD scans of the GaNAs and GaNAsSb showed that temperature did have an effect on the composition (and thus strain and structure) of the material.

When the substrate temperature was increased, the strain in the GaNAsSb samples shifted from slightly compressive to slightly tensile. It is suspected that the shift in strain is probably due to a reduction in Sb since it is known that Sb tends to desorb more readily at higher growth temperatures. To determine whether or not temperature has an effect on N incorporation, GaNAs was grown with varying substrate temperatures as well. From HRXRD scans, it was seen that the N composition remained the same, except for the hottest sample in which there was a slight decrease in N. The most surprising result from the HRXRD scans was the fact that the samples did not appear to have any significant segregation, relaxation or interface degradation when grown at higher temperatures. All samples had very well defined QW peaks and Pendellosung fringes. To confirm that the (004) $\omega/2\theta$ scans were not missing any signs of relaxation or segregation, reciprocal space maps (RSMs) were taken of the (224) directions of GaNAs and GaNAsSb. RSMs show the in-plane and perpendicular components of diffraction and the lattice spacing of the material present. There are no major diffraction peaks in the in-plane direction away from the (224) GaAs peak. Figure 5 is a plot of SIMS scans taken of the GaNAsSb samples to measure composition and depth profiles. As seen in the Figure, there is a large decrease in Sb concentration with increasing substrate temperature, while the N concentration remained roughly constant. The loss of 8% Sb explains the large shift in the strain observed in HRXRD peaks. Similar to the SIMS data from the As overpressure study, the N composition remained constant, even though the Sb concentration changed. With this data, one might be encouraged by the fact that at high temperatures the material obtained was coherent and had smaller amounts of Sb, so that the bandgap was larger. However, the PL results were very unexpected given the previous results and quickly destroyed any notion that high temperature was advantageous. In addition to the loss of PL intensity, there was also a large shoulder on the long wavelength side for all three samples which was not found in the original substrate temperature sample. This longer wavelength shoulder could be a result of microsegregation which could not be observed easily in HRXRD. Since there could be areas of clustering of increased N concentration within the QW, it could lead to areas of luminescence in which the bandgap is smaller, leading to luminescence at longer wavelength. If these regions occurred only inside the QWs, they would have no effect on the interfaces and thus would not affect or reduce the diffraction thickness oscillations. As evidenced by the poor PL results, GaNAsSb cannot be grown at high temperatures without a large decrease in optical material quality.

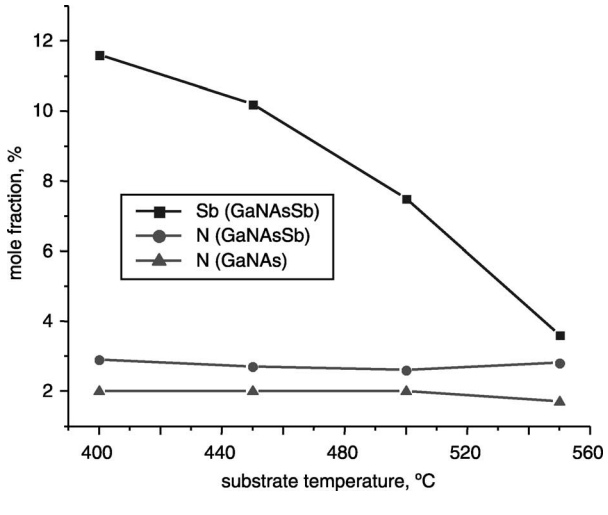

Fig. 5 *SIMS results of N and Sb for GaNAs and GaNAsSb as a function of substrate temperature*

In choosing a barrier material for a QW, it is desirable to have certain key properties which will enhance the structure without detrimental effects. The barriers must have type-I alignment and have sufficient band-offset to localise the electrons and holes in the QW. If the QW is strained, it would be important to strain-compensate with barriers of the opposite sign strain. This will prevent relaxation and the formation of defects by effectively increasing the critical thickness of the layers. Finally, the material must be of good quality or defects present will lead to a higher rate of nonradiative recombination, preventing carriers from radiatively recombining in the QW. One of the limitations of MBE is the inability to accurately change fluxes during growth, but most MBE systems do not have this capability. GaNAs was the previous barrier material utilised in GaInNAs QWs [11, 15, 25]. When Sb was added to GaInNAs, Sb was also added to GaNAs, assuming that the expected surfactant nature of Sb and the improvement in material to GaInNAs would also apply to GaNAs. However, the GaNAsSb material has several properties which do not make it the desired barrier material of choice. Examination of RHEED patterns showed that the addition of Sb to GaNAs actually degraded the surface quality and turns the pattern from streaky to spotty. This suggests that the surface roughens and there could be clustering on the surface which could lead to defects. GaNAsSb does not provide any strain compensation to the highly compressive GaInNAs(Sb) QWs. Without strain compensation, it is difficult to grow more than 1–2 QWs in a laser structure, a serious limitation for high-power laser diodes or VCSELs. GaNAs, however, is tensile and does provide strain compensation. The GaNAsSb barriers used for GaInNAs(Sb) QWs also have a bandgap value which is very close to that of the QW. Having a small band-offset in the valence and conduction bands results in poor hole and electron confinement and may even reduce the overlap between the two wavefunctions. This would lead to poor luminescence and also poor thermal characteristics in device performance. It is also suspected that GaNAsSb has a bandgap region which is shifted towards the conduction band edge, since Sb tends to increase valence band-offsets while not affecting the conduction band-offset. This could lead to a type-II alignment with the QW. GaNAs has a larger bandgap ($\sim$1.1–1.2 eV) and thus provides better electron and hole confinement. Finally, the optical properties of GaNAsSb have been found to be of relatively poor quality. Although PL is not the absolute measure of optical and electrical quality of a material, it does give a very good idea. From these findings, it is seen that GaNAs is the better barrier material compared to GaNAsSb for GaInNAs(Sb) QWs.

The device structures reported in Sections V and VI for our long-wavelength GaInNAs(Sb) optoelectronic devices were changed to reflect the new knowledge that GaNAs was a superior barrier material. This change led to an improvement in GaInNAsSb PL quality. For GaInNAsSb QW samples at 1.55 μm, the FWHM of the PL peak was 57 meV with GaNAsSb barriers and 44 meV with GaNAs barriers. The FWHM of the PL peak is a good measure of the quality of the material and structure. Once it was confirmed that the PL quality improved, edge-emitting lasers and VCSELs were grown with the new device structure.

4 Plasma-source ion damage

A second critical growth issue is the potential for ion or electron damage from the RF plasma source used in MBE systems to produce a reactive N species. Nitrogen is difficult to incorporate into GaAs, with an equilibrium solubility $< 0.5\%$. GaNAs and related dilute nitride materials must be grown under non-equilibrium conditions by MBE or OMVPE. In the case of MBE, a RF N plasma source is used to supply atomic N for the growth, and alloys with up to 10% N have been grown. There is little quantitative knowledge of exactly what species are being generated in such RF plasma sources, with N, N_2^+, N^2 radicals and electrons being the most prevalent. As a result, there has always been a question of whether N_2^+ ions or electrons do any damage to the growing epitaxial materials. Another key question is whether radicals incorporate as N–N pairs or as a N interstitial or $[N]_{Ga}$ antisite.

There are various methods that can be used to remove ions from the output of a plasma source. The earliest of these was to apply magnets to the plasma, causing charged ions to travel a curved path. This was used in ECR plasma sources for GaN [26]. Another technique is to use a set of dense metal meshes with different voltages, to repel charged species. This has been useful for studies of the plasma condition, but has not been reported as a growth technique due to the restriction in the beam path and, presumably, the risk of sputtering undesirable metal ions from the mesh onto the wafer. Other techniques include biasing the substrate or ion collection within the cell. The RF power and gas flow rate have a strong effect on the fraction of ions in the output of the plasma source, with low RF power and high flow giving the fewest ions but also the least atomic N. Similarly, we verified that using smaller or fewer holes in the aperture at the end of the plasma source decreased plasma damage and improved the stability of the plasma [11, 25].

Another common technique is to add high-voltage ion deflection plates. These are simply parallel, metal plates on either side of the output beam of the plasma. If a bias is applied across the two plates, the electric field will drive positive ions in one direction and electrons in the opposite direction. Negative ions are assumed to be negligible. We initially applied ± 800 V to the deflection plates for 1600 V total bias and found no consistent improvement in photoluminescence of GaInNAs [25]. We now believe that such a high-voltage bias may have ionised additional N through a DC-enhanced plasma in front of the source, or it may have caused sputtering of metal or adsorbed contaminants from the deflection plates which landed on the wafer. We were not able to measure the current through the deflection plates, as the RF coupled excessive noise into the picoammeter. Furthermore, if the deflection plates are not equally and oppositely biased, then they provide a potential barrier to either electrons or positive ions. For example, if one deflection plate were biased to $+30$ V and the other to -10 V, there would be a net $+10$ V potential which would tend to repel ions. This observation is significant for high biases, because high-voltage power supplies are not necessarily accurate to within a volt, and if there exists a few volts' difference between the two deflection plates, it could lead to a change in ion extraction from the plasma. It should be noted that the repulsion is not necessarily one-to-one, partly due to the finite size of the deflection plates, and partly due to the screening provided by the electrons. Because only one set of deflection plates is available in our system, the plasma is affected by the net potential on the deflection plates. A negative potential would extract additional positive ions from the plasma cell, and *vice versa*, assuming that the plasma is in good electrical contact with the grounded pipe at the rear of the source. Also, because electrons are believed to be less damaging than ions, a net positive bias should prevent most damage to the wafer.

One of the features of most MBE systems is that a nude ion gauge is mounted on the backside of the substrate holder to measure beam fluxes before growth. This is illustrated in Fig. 6, where the sample is in the growth position at the top and the ion gauge facing the N source at the bottom. By rotating the ion gauge up and down slightly and with different biases on the filament, one can produce a reasonable spatial map and energy distribution for both electrons and ions from the source. By measuring the location of peak electron current, we were able to demonstrate that small voltages physically deflect the ions and electrons to different locations, as shown in Fig. 7. The solid line shows the suggested relation between the position of the peak ion flux (which is thermally broadened) and the voltage on the upper deflection plate. The lower deflection plate was grounded for this experiment. The deviation from the solid line from -20° to -30° was due to shadowing of the ion gauge collector wire by the thicker filament wire in front of it. The deviation to the right of $+18^\circ$ was due to blocking of the plasma beam by a protective bracket on the beam flux monitor. Also, the axis of motion of the ion gauge was vertical, but the axis of the deflection plates was about 45° from vertical, so the ion deflection has a horizontal component as well as a vertical one. At larger angles this

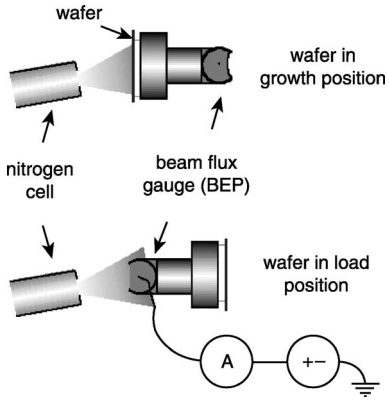

Fig. 6 *Schematic of MBE substrate holder/beam flux monitor and its use to measure ion/electron currents from RF N plasma source*

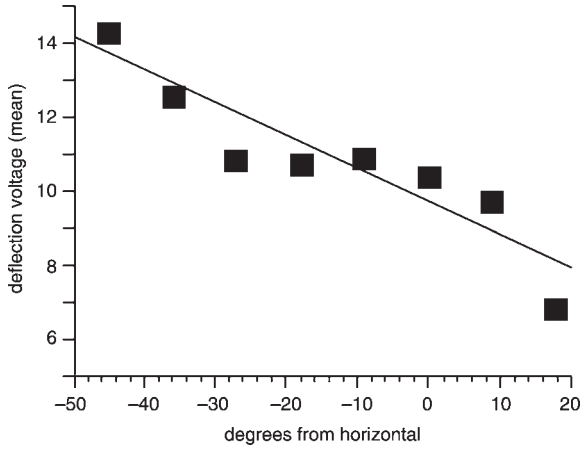

Fig. 7 *Deflection of ions with applied bias on a single deflection plate*

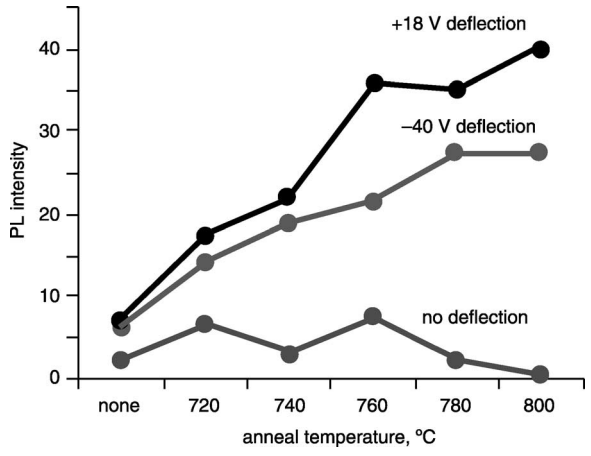

Fig. 8 *Photoluminescence for samples grown with different voltages applied to one deflection plate*

The other plate was grounded. Note the higher luminescence over all annealing conditions, and the higher anneal temperatures reachable before the PL is quenched

deflection could cause the ions to miss the gauge completely. These geometric complications prevented a simple quantification of the ion energy, but nevertheless indicate that complete deflection of ions from our plasma source does not require particularly high voltages.

Following the successful mapping of the electron and ion distributions with deflection plate bias, we set off to test the hypothesis that minimising the ion current and, hence, damage would result in better material. We grew three samples with biases of +18 V, 0 V and −40 V applied to one deflection plate for the respective samples. The other plate was grounded for all three samples. Each sample was a single 7-nm GaInNAsSb quantum well with GaNAs barriers. Figure 8 shows the PL intensity as a function of anneal temperature for these three samples. The PL not only shows very clear improvement with deflection bias, but that improvement appears to keep rising to the highest anneal temperature or time. This is in complete contrast to all our materials grown without deflection plate bias which peak at some anneal temperature/time and then decrease when either of these is exceeded. At high anneal temperatures, the sample with +18 V deflection had more than 5 times greater PL intensity and at low pump powers, the relatively narrow PL linewidth was reduced even further with deflection bias and PL linewidth of 32 meV was observed after 800 °C anneal.

5 GaInNAs high-power edge-emitting lasers

The challenges for achieving luminescence and lasing beyond 1.3 μm were illustrated in Fig. 3 before the addition of Sb. With the addition of Sb, we were able to achieve strong PL out to 1.6 μm, hence we initiated growth and fabrication of edge-emitting lasers to operate at 1.5 μm. With the improved growth conditions (low temperature, deflection plate bias and GaNAs barriers), single QW PL samples exhibited a room-temperature (RT) PL peak at 1.42 μm and a linewidth of 29.7 meV. This is the narrowest PL linewidth reported for such QW structures, an indication of the much improved growth conditions for these PL samples and resulting lasers [7].

Lasers were grown on (100) n-type GaAs substrates. Solid silicon and CBr_4 sources were used for n- and p-type doping, respectively. The active layer was a single, 7-nm GaInNAsSb QW surrounded by 20-nm-thick GaNAs barriers. The QW active region was embedded in the centre of a one-wavelength undoped GaAs waveguide surrounded by $Al_{0.3}Ga_{0.7}As$ cladding layers. The structure was capped with a highly p^+-doped GaAs contact layer. Device fabrication consisted of lift-off metallisation (Ti/Pt/Au) followed by a self-aligned dry etch through the top $Al_{0.3}Ga_{0.7}As$ cladding layer. The wafers were thinned to 120 μm to allow the cleavage of high-quality mirrors and backside metal (AuGeNi/Au) was evaporated. This was followed by a one-minute contact sinter at 410 °C. Device bars ranging in length from 400–800 μm were manually cleaved.

Figure 9*a* shows the CW RT light output with input current (L–I) for a device measuring 20 × 760 μm. The device lased at 1.490 μm (Fig. 9*b*) with a CW threshold of 1.1 kA/cm^2. The CW slope efficiency was 0.34 W/A, corresponding to 40% external quantum efficiency. These are the best threshold current density and efficiency data reported for a dilute-nitride laser operating at $\lambda > 1.4$ μm [6, 7]. These devices showed maximum CW

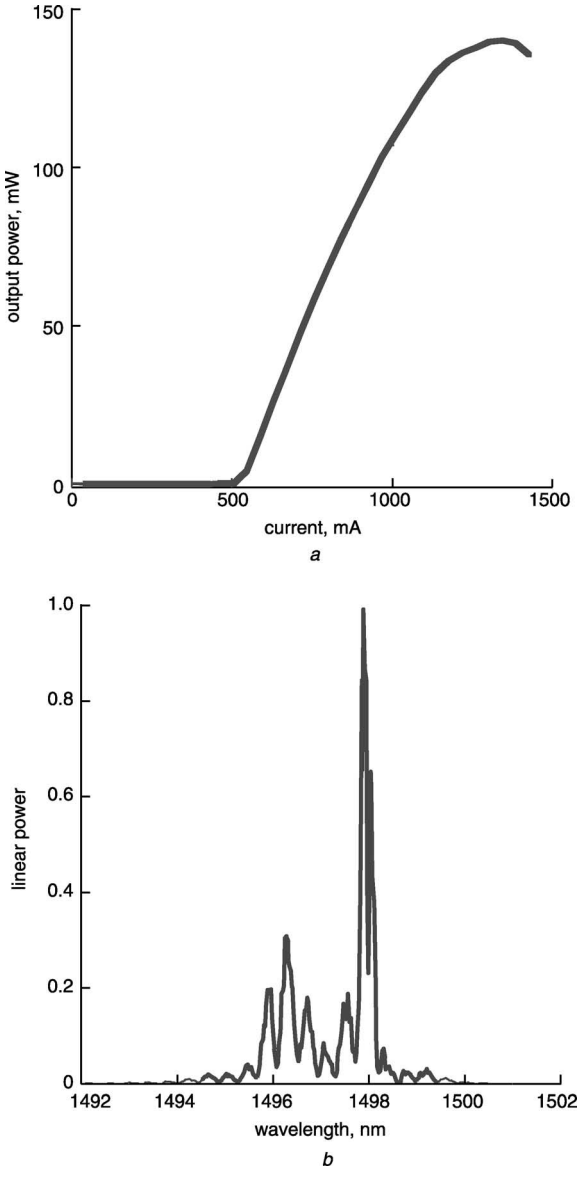

Fig. 9 *Light output power and emission spectra of 20-μm-wide × 2450-μm-long ridge waveguide edge-emitting laser for CW operation at room temperature*

a Light output power against injection current (L–I) characteristic
b Emission spectra at 600 mA ($\sim 1.2\,I_{th}$)

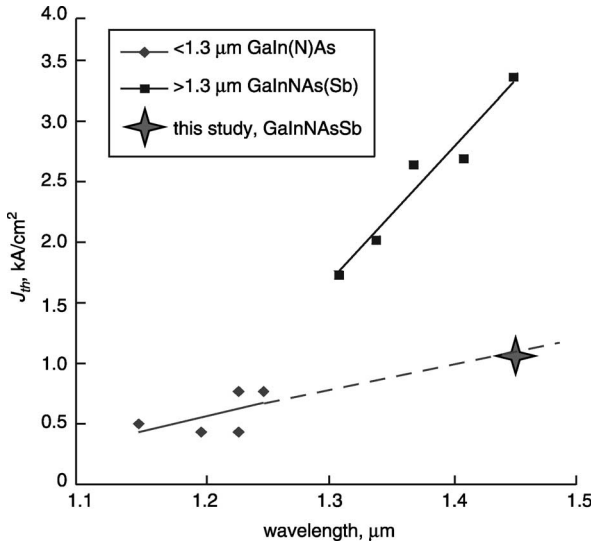

Fig. 10 *Threshold current of GaInNAs lasers ($1.15 < \lambda < 1.25\,\mu m$) from several groups and our earlier GaInNAsSb lasers ($\lambda > 1.30\,\mu m$) and most recent result at 1.46 μm with optimised growth conditions*

output powers of 30 mW before thermal rollover and pulsed output powers (5 μs pulse, 1% duty cycle) as high as 300 mW. The device structure was chosen to minimise thermal heating around the active layer to allow CW operation. A difference of 200 A/cm^2 between pulsed and CW threshold current density indicates some heating, although other devices showed significantly less difference.

The turn-on voltage was 0.9 V, which compares favourably with the bandgap energy of 0.83 eV. Additionally, the diode ideality factor was computed to be 1.3. These data indicate an excellent balance between device heating issues and free carrier absorption. A comparison of devices from several groups for lasers with $\lambda > 1.25\,\mu m$ is shown in Fig. 10. The significant improvement in materials technology is clearly evident in the factor of three lower threshold current density compared to other reported devices at comparable wavelengths. While the threshold current is very impressive, these devices are more temperature sensitive. The characteristic temperature (T_o) under pulsed conditions was 62 K as measured in the range 25–60 °C. This is probably due to reduced electron confinement in GaInNAsSb/GaNAs structures as compared to GaInNAs/GaAs [6] structures and will be tested in the near future.

6 GaInNAs long wavelength VCSELs

The VCSELs consist of a bottom mirror, top mirror and one lambda cavity with three QWs. The bottom mirror consisted of 29 alternating pairs of silicon-doped $Al_{0.92}Ga_{0.08}As$ and GaAs, making a distributed Bragg reflector (DBR). The cavity was a one-lambda-thick layer of GaAs, designed for 1.485 μm, with three quantum wells (QWs) at the centre. The QW were based on edge-emitting lasers which operated at wavelengths from 1.49–1.51 μm. The QWs were 7-nm $Ga_{0.62}In_{0.38}N_{0.016}As_{0.958}Sb_{0.026}$ with 20-nm GaNAs barriers below, between and above the QWs. The compositions were determined from calculations based on SIMS, XRD, RBS and NRA–RBS. The top DBR was p-doped with carbon and 24 pairs thick. A thin, digital alloy of 98% aluminium was included as part of the second AlGaAs layer from the cavity. N was supplied by an SVT Associates RF plasma cell at 300 W and 0.5 sccm. The Sb flux was 1.15×10^{-7} torr and the As overpressure was 20 times the group-III flux in the quantum wells and 15 times elsewhere. Because the nitride MBE system did not have enough ports for multiple AlGaAs compositions, the DBRs were grown in a separate, but connected, MBE system and transferred under ultrahigh vacuum. Plasma conditions were optimised to minimise plasma damage during growth. A conventional liftoff process was used to define metal rings for the top contacts, and top and bottom metal was deposited in an evaporator. Unfortunately, the liftoff failed to remove the metal at the centre of each mesa until the metal was thinned using aqua regia (1:3 HNO_3:HCl). This step significantly damaged the metal and the wafer surface, leading to rough sidewalls and surfaces, adding significant scattering loss to the VCSELs. Even with the aqua regia etch, very few mesas smaller than 62 μm in diameter lifted off. Also, because the selective oxidation layer was too thin, it did not significantly oxidise, so rather than a single current-confining layer, the top DBR oxidised uniformly about 10 μm inwards. This added optical scattering losses and series resistance to the top DBR. In spite of these processing difficulties, some lasers survived to be tested. The VCSELs were mounted epi-side-up on a copper chuck, and cooled by a thermoelectric cooler (TEC), for testing.

Despite all the above difficulties, the VCSELs lased in pulsed mode when cooled to a chuck temperature of −10 °C. Figure 11 shows the fibre-coupled power, as a function of wavelength, at 500 mA and 800 mA of peak current, showing the onset of stimulated emission. The VCSELs were pulsed at 0.1% duty cycle, with 2 μm pulses at a 500 Hz repetition rate. Multiple transverse modes are visible above threshold, due to the large 66 μm current aperture size of the VCSELs. The threshold current I_{th} was 543 mA (pulsed), corresponding to current density J_{th} of 16 kA/cm^2, or 5.3 kA/cm^2 per QW. The VCSEL QWs were identical to the single quantum well from our earlier CW 1.49 μm edge-emitting lasers. Owing to the lower operating temperature and a short cavity, the VCSELs lased at 1.46 μm, a significantly shorter wavelength. Microcavity emission from a similar structure showed that the growth of the top DBR only partially annealed the active region, but an additional rapid thermal anneal was required for peak photoluminescence. Several other devices produced up to 33 μW peak power. This modest power is surprisingly high

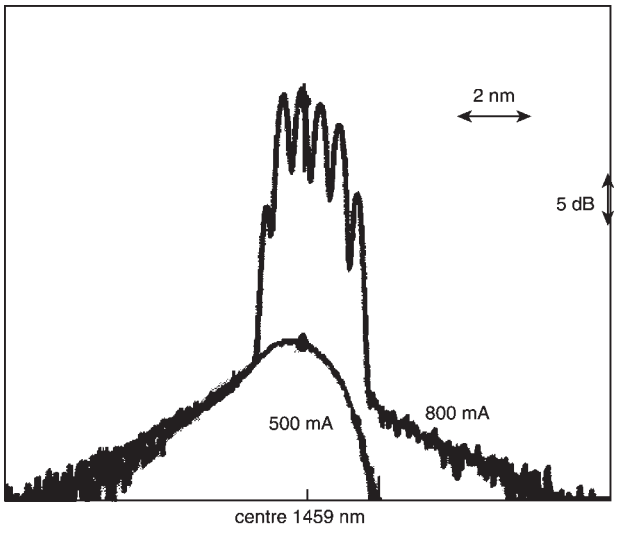

Fig. 11 *Spectra of the first monolithic $\lambda > 1.45\,\mu m$ VCSEL on GaAs operating just below and about 1.6 times threshold*

given the problems outlined above and the mismatch between the cavity resonance and the actual emission wavelength (gain peak). It is expected that better mounting techniques will reduce the need for such low cooling temperatures.

7 Summary

The key challenge for expansion of wide bandwidth communications to the desktop is to greatly reduce the cost of lasers and monolithic integration of all components into photonic integrated circuits. We believe that GaInNAsSb on GaAs will be the foundation technology that will enable low-cost, wide bandwidth MAN/LAN/SAN networks, optical switching and routers. Dilute nitride GaInNAsSb grown epitaxially on GaAs can produce active quantum well regions that cover the full 1.2–1.6 μm wavelength region with a single alloy material system. This not only greatly simplifies processing, but enables incorporation of the tremendous processing advantage of oxidised AlAs to form high-index-contrast photonic crystal structures as well as the existing AlAs/GaAs DBR mirror and VCSEL manufacturing technology. This will become an enabling technology not only for long wavelength lasers, but also for advanced photonic integrated circuits.

The major challenge of this material system has been to understand the differences of dilute nitrides compared to other III–V alloys and to produce low-threshold lasers at any desired wavelength between 1.3 and 1.6 μm. The most recent results incorporating Sb to form a quinary alloy GaInNAsSb appear to overcome many of the prior problems involving phase segregation, and understanding the role of damage from plasma sources has dramatically reduced the threshold current of long wavelength lasers. We believe that GaInNAsSb will be the active gain material of choice because it has significantly higher gain for VCSELs, is closer to the existing QW technologies than InAs QDs and has fundamental energy band advantages over its other competitors. GaInNAsSb also has an inherent lateral uniformity advantage over other active QW material choices. However, this is only realised by solid-source MBE because of the relative compositional insensitivity to As flux and temperature. While MBE has been utilised for production of very-low-cost, edge-emitting CD-lasers, it has not been utilised in the production of VCSELs, although it has been the tool of choice for most of the research and development of VCSELs. The newest versions of production MBE systems with their greater versatility in number of liquid metal sources could easily change the role of MBE. The advances in equipment combined with the significantly easier growth of GaInNAsSb by MBE will probably make MBE the choice for production of VCSELs, high-power edge-emitting lasers and photonic integrated circuits. Progress has been fast and furious and the future for this materials system and the potential for its inclusion as a major part of the optical networks is indeed bright.

8 Acknowledgments

This work has been the result of efforts by a number of truly great graduate students, including the coauthors and V. Lordi, T. Gugov, H. Bae, L. Goddard, V. Gambin, W. Ha, S. Spruytte, C. Coldren, M. Larson and Dr. K. Volz. The authors would also like to thank Dr. A. Moto, Sumitomo Electric, for substrates, SIMS and helpful discussions, Prof. A. Adams at University of Surrey for helpful discussions on absorption, carrier leakage and recombination mechanisms and S. Smith, Charles Evans & Associates for SIMS profiles. This work was supported both financially and technically by Drs B. Leheny and E. Towe at DARPA and Drs Y.-S. Park and C. Wood at ONR over a number of years through the Optoelectronics Materials Center, contracts MDA972-00-1-0024, DARPA/ARO contract DAAG55-98-1-0437, ONR contract N00014-01-1-0010, the MARCO Interconnect Focus Center and the Stanford Network Research Center.

9 References

1 Harris, J.S., Jr.: 'GaInNAs long wavelength lasers: progress and challenges', *Semicond. Sci. Technol.*, 2002, **17**, pp. 880–891 and references therein
2 Harris, J.S., Jr.: 'GaInNAs and GaInNAsSb long wavelength lasers', in Buyanova, I., and Chen, W. (Eds.): 'Physics and applications of dilute nitrides' (Taylor and Francis, London, UK, 2004), and chapters therein
3 Harris, J.S., Jr.: 'Tunable long-wavelength vertical-cavity lasers: the engine of next generation optical networks?', *IEEE J. Sel. Top. Quantum Electron.*, 2000, **6**, pp. 1145–1160
4 Kondow, M., Uomi, K., Niwa, A., Kitantai, T., Watahiki, S., and Yazawa, Y.: 'GaInNAs: a novel material for long-wavelength-range laser diodes with excellent high-temperature performance', *Jpn. J. Appl. Phys.*, 1996, **35**, pp. 1273–1275
5 Kisker, D.W., Chirovsky, L.M.F., Naone, R.L., Van Hove, J.M., Rossler, J.M., Adamcyk, M., Wasinger, N., Beltran, J.G., and Galt, D.: '1.3 mm VCSEL production issues'. Proc. SPIE Photonics West Conf., San Jose, CA, USA, Jan. 2004 (SPIE, Bellingham, WA, 2004)
6 Ha, W., Gambin, V., Bank, S., Wistey, M., Yuen, H., Kim, S., and Harris, J.S., Jr.: 'Long-wavelength GaInNAs(Sb) lasers on GaAs', *IEEE J. Quantum Electron.*, 2002, **38**, pp. 1260–1267
7 Bank, S.R., Wistey, M.A., Yuen, H.B., Goddard, L.L., Ha, W., and Harris, J.S., Jr.: 'Low-threshold CW GaInNAsSb/GaAs laser at 1.49 μm', *Electron. Lett.*, 2003, **39**, pp. 1445–1446
8 Wistey, M.A., Bank, S.R., Yuen, H.B., Goddard, L.L., and Harris, J.S.: 'Monolithic, GaInNAsSb VCSELs at 1.46 μm on GaAs by MBE', *Electron. Lett.*, 2003, **39**, pp. 1822–1823
9 Kovsh, A.R., Wang, J.S., Wei, L., Shiao, R.S., Chi, J.Y., Volovik, B.V., Tsatsul'nikov, A.F., and Ustinov, V.M.: 'Molecular beam epitaxy growth of GaAsN layers with high luminescence efficiency', *J. Vac. Sci. Technol. B, Microelectron. Nanometer Struct.*, 2002, **20**, pp. 1158–1162
10 Wistey, M.A., Bank, S.R., Yuen, H.B., and Harris, J.S.: 'Low voltage deflection plates reduce damage to GaInNAs from a nitrogen rf plasma', submitted to *Appl. Phys. Lett.*
11 Spruytte, S.G., Larson, M.C., Wampler, W., Coldren, C.W., Petersen, H.E., and Harris, J.S.: 'Nitrogen incorporation in group III-nitride-arsenide materials grown by elemental source molecular beam epitaxy', *J. Crystal Growth*, 2001, **227–228**, pp. 506–515
12 Hasse, A., Volz, K., Schaper, A.K., Koch, J., Höhnsdorf, F., and Stolz, W.: 'TEM investigations of (GaIn)(NAs)/GaAs multi-quantum wells grown by MOVPE', *Cryst. Res. Technol.*, 2000, **35**, pp. 787–792
13 Shimizu, H., Kumada, K., Uchiyama, S., and Kasukawa, A.: '1.2 μm range GaInAs SQW lasers using Sb as surfactant', *Electron. Lett.*, 2000, **36**, pp. 1379–1381
14 Yang, X., Heroux, J.B., Mei, L.F., and Wang, W.I.: 'InGaAsNSb/GaAs quantum wells for 1.55 μm lasers grown by molecular-beam epitaxy', *Appl. Phys. Lett.*, 2001, **78**, pp. 4068–4070
15 Bank, S.R., Ha, W., Gambin, V., Wistey, M.A., Yuen, H.B., Goddard, L.L., Kim, S.M., and Harris, J.S., Jr.: '1.5 μm GaInNAs(Sb) lasers grown on GaAs by MBE', *J. Cryst. Growth*, 2003, **251**, pp. 367–371
16 Li, L.H., Sallet, V., Patriarche, G., Largeau, L., Bouchoule, S., Merghem, K., Travers, L., and Harmand, J.C.: '1.5 μm laser on GaAs with GaInNAsSb quinary quantum well', *Electron. Lett.*, 2003, **39**, pp. 519–520
17 Ungaro, G., LeRoux, G., Teisseir, R., and Harmand, J.C.: 'GaAsSbN: a new low-bandgap material for GaAs substrates', *Electron. Lett.*, 1999, **35**, pp. 1246–1248
18 Harmand, J.C., Ungaro, G., Largeau, L., and LeRoux, G.: 'Comparison of nitrogen incorporation in molecular-beam epitaxy of GaAsN, GaInAsN, and GaAsSbN', *Appl. Phys. Lett.*, 2000, **77**, pp. 2482–2484
19 Volz, K., Gambin, V., Ha, W., Wistey, M.A., Yuen, H.B., Bank, S.R., and Harris, J.S., Jr.: 'The role of Sb in the MBE growth of (GaIn)(NAsSb)', *J. Cryst. Growth*, 2003, **251**, pp. 360–366
20 Sun, X., Wang, S., Hsu, J., Sidhu, R., Zheng, X., Li, X., Campbell, J., and Holmes, A., Jr.: 'GaAsSb: a novel material for near infrared photodetectors on GaAs substrates', *IEEE J. Sel. Top. Quantum Electron.*, 2002, **8**, p. 817
21 Tournie, E., Grandjean, N., Trampert, A., Massies, J., and Ploog, K.: 'Surfactant-mediated molecular-beam epitaxy of III–V strained-layer heterostructures', *J. Cryst. Growth*, 1995, **150**, pp. 460–466
22 Gambin, Lordi, V., Ha, W., Wistey, M., Takizawa, T., Uno, K., Friedrich, S., and Harris, J.S., Jr.: 'High intensity 1.3–1.6 μm

luminescence and structural changes on anneal from MBE grown (GA, In)(N, As, Sb)', *J. Cryst. Growth*, 2003, **251**, pp. 408–411
23 Lordi, V., Gambin, V., Friedrich, S., Funk, T., Takizawa, T., Uno, K., and Harris, J.S., Jr.: 'Nearest-neighbor configuration in (GaIn)(NAs) probed by x-ray absorption spectroscopy', *Phys. Rev. Lett.*, 2003, **90**, pp. 145505–145507
24 Klar, P., Gruning, H., Koch, J., Schafer, S., Volz, K., Stolz, W., Heimbrodt, W., Saadi, A., Lindsay, A., and O'Reilly, E.: '(InGa)(NAs)-fine structure of the band gap due to nearest-neighbor configurations of the isovalent nitrogen', *Phys. Rev. B, Condens. Matter Mater. Phys.*, 2001, **64**, pp. 121203–121206
25 Gambin, V., Ha, W., Wistey, M., Bank, S., Yuen, H., Kim, S., and Harris, J.S., Jr.: 'GaInNAsSb for 1.3-1.6 μm long wavelength lasers grown by molecular beam epitaxy', *IEEE J. Sel. Top. Quantum Electron.*, 2002, **8**, pp. 795–800
26 Molnar, R.J., and Moustakas, T.D.: 'Growth of gallium nitride by electron-cyclotron resonance plasma-assisted molecular-beam epitaxy: the role of charged species', *J. Appl. Phys.*, 1994, **76**, pp. 4587–4595